UDK 669.14.018.8.: 669.193
Original scientific article/Izvirni znanstveni članek

ISSN 1580-2949
MTAEC9, 45(2)91(2011)

A COMPARISON OF THE CORROSION BEHAVIOUR OF AUSTENITIC STAINLESS STEELS IN ARTIFICIAL SEAWATER

PRIMERJAVA KOROZIJSKIH LASTNOSTI AVSTENITNIH NERJAVNIH JEKEL V SIMULIRANI MORSKI VODI

Aleksandra Kocijan

Institute of Metals and Technology, Lepi pot 11, SI-1000 Ljubljana, Slovenia
aleksandra.kocijan@imt.si

Prejem rokopisa – received: 2011-03-15; sprejem za objavo – accepted for publication: 2011-03-25

The evolution of the passive films formed on AISI 317LNM and AISI 316L stainless steels in artificial seawater was studied using the electrochemical techniques of cyclic voltammetry and potentiodynamic measurements. The extent of the passive range increased significantly for the AISI 317LNM stainless steel compared to the AISI 316L in the investigated solution. The cyclic voltammograms of the AISI 317 LMN and AISI 316L were recorded in artificial seawater. The current-density peaks formed during the cyclic voltammetry were ascribed to the corresponding electrochemical processes taking place on the surface of the investigated materials, and the influence of the potential scan rate was also studied. The current density of the peaks increased linearly with the scan rate. The potentials of the anodic and cathodic peaks moved slightly, with the increasing scan rate, towards more positive and negative values, respectively.

Keywords: stainless steel, sea water, chloride, cyclic voltammetry, potentiodynamic measurements

Z elektrokemijskimi tehnikami ciklične voltametrije in potenciodinamskih meritev smo raziskovali tvorbo pasivne plasti na površini nerjavnih jekel AISI 317LNM in AISI 316L v raztopini simulirane morske vode. Širina pasivnega območja je pri nerjavnem jeklu AISI 317 LMN bistveno večja kot pri AISI 316L v preiskovani raztopini. S ciklično voltametrijo smo opisali nastale vrhove s procesi, ki potekajo na površini preiskovanih vzorcev. Raziskovali smo tudi vpliv spreminjanja potenciala s časom na obliko cikličnih voltamogramov. Ugotovili smo, da z naraščajočo hitrostjo spreminjanja potenciala s časom prihaja do rahlega naraščanja in premika vrhov.

Ključne besede: nerjavno jeklo, morska voda, kloridi, ciklična voltametrija, potenciodinamske meritve

1 INTRODUCTION

The austenitic stainless steel AISI 316L is one of the most commonly used materials. Its mechanical properties, such as ductility and wear resistance, make it attractive for particular applications. The corrosion resistance of stainless steel is relatively good. However, it is challenged by the hostile environment in marine applications, as it is susceptible to localised corrosion in environments containing chloride [1].

The austenitic stainless steel AISI 317LNM is a nitrogen-alloyed austenitic stainless steel with a high molybdenum addition. It exhibits an austenitic microstructure free of deleterious carbide precipitations at the grain boundaries. The grade contains some residual ferrite, up to 2 % after solution annealing at temperatures 1100–1150 °C and water quenching. Its low carbon content avoids the intergranular corrosion, even on welded pieces without an ulterior water quenching. The high molybdenum content gives this steel a higher resistance to corrosion in chloride-containing environments than standard grades, i.e., AISI 316L. Nitrogen additions and a low silicon content have a stabilizing effect on the austenitic structure, reducing the precipitation of inter-metallic phases during welding. The nitrogen addition also increases the yield strength compared to AISI 317L. Its main properties are a high ductility, an easy weldability and a high corrosion resistance. The main applications are chemical and petrochemical applications, pollution control equipment and chemical tankers [2].

Several techniques have been used to study the corrosion behaviour of stainless steels in different media [1,3–27]. The behaviour of AISI 316L stainless steel in chloride-containing solutions has been studied by various authors [28–31]. Platt et al. [28] compared the corrosion behaviour of 2205 duplex stainless steel and AISI 316L in a 0.9 % chloride solution. Electrochemical testing indicated that the 2205 duplex stainless steel had a wider passivation range than the AISI 316L. Blanco et al. [29] investigated the corrosion behaviour of two traditional austenitic stainless steels in reinforced concrete structures exposed to highly chloride-contaminated atmospheres. The effects of ion nitriding on the corrosion performance of a 316L stainless steel were evaluated in a 0.9 % sodium chloride solution by Gil et al. [30]. It was shown that an ion nitriding treatment in a 25 % N_2–75 % H_2 atmosphere performed at a temperature of 410 °C improves the surface hardness of the AISI 316L stainless steel. However, under the experimental conditions carried out in this research, the nitrided steel is as prone to localized corrosion as the untreated one. It is consi-

dered that this behaviour is mainly due to the presence of CrN, which precipitates during processing, contributing to the depletion of chromium from the adjacent matrix and leading to a galvanic corrosion mechanism. Hryniewicz et al. [31] compared the corrosion behaviour of austenitic stainless steels after two electropolishing processes carried out in the absence and presence of a magnetic field. It has been shown that the proposed magnetic field process shifts the corrosion potentials in the direction of greater corrosion resistance.

The influence of artificial seawater on the corrosion properties of AISI 317LMN stainless steel has not been investigated extensively. Among the more recent work, only one paper concerning the corrosion resistance of AISI 317LMN stainless steel for an application in pre-stressed concrete structures was published [2].

In the present work AISI 317LMN stainless steel and AISI 316L stainless steel were studied in artificial seawater. The study was conducted using the electrochemical techniques of cyclic voltammetry and potentiodynamic measurements.

2 EXPERIMENTAL

AISI 317 LMN stainless steel and AISI 316L stainless steel were investigated. Their compositions were confirmed by analytical chemical methods, as shown in **Table 1**. The concentrations of Cr, Ni, Mn and Mo were determined by using inductively coupled plasma atomic emission spectroscopy (ICP-AES, ICP-AES Perkin Elmer Optima 3100 RL instrument), the concentration of Si was determined gravimetrically (Mettler H35AR balance). A spectrophotometric method using the bismuth phosphomolybdate complex was applied for the determination of phosphorus. A blue complex formed was extracted with methyl isobutyl ketone. The absorbance was measured at 625 nm (Opton PM 6 spectrophotometer). The concentration of carbon was determined by the oxidation of the sample in an induction furnace by heating in an oxygen atmosphere to form CO2, which was then measured with an infrared detector (Eltra CS-800 instrument). The measuring principle is based on the infrared-radiation-absorbing properties of the gases. In the case of the nitrogen determination the sample was melted at high temperatures up to 3000 °C in an electrically heated graphite crucible in the furnace. The concentration of nitrogen was determined with a thermal conductivity detector (Eltra ON-900 instrument).

The experiments were carried out in artificial seawater with a composition of 3.5 % NaCl (Merck, Darmstadt, Germany).

The test specimens were cut into discs of 15 mm diameter. The specimens were ground with SiC emery paper down to 1000 grit prior to the electrochemical studies, and then rinsed with distilled water. The specimens were then embedded in a Teflon PAR holder and employed as a working electrode. The reference electrode was a saturated calomel electrode (SCE, 0.242 V vs. SHE) and the counter electrode was a high-purity graphite rod.

The cyclic voltammetry and potentiodynamic measurements were recorded using an EG&G PAR PC-controlled potentiostat/galvanostat Model 273 with M252 Softcorr III computer programs. In the case of potentiodynamic measurements the specimens were immersed in the solution 1 h prior to the measurement in order to stabilize the surface at the open-circuit potential. The potentiodynamic curves were recorded, starting at 250 mV more negative than the open-circuit potential. The potential was then increased, using a scan rate of 1 mV/s, until the transpassive region was reached.

3 RESULTS AND DISSCUSION

The potentiodynamic behaviour of AISI 317LMN and AISI 316L stainless steels in artificial seawater is shown in **Figure 1**. The differences in the alloys' compositions affected the polarisation and the passivation behaviours of the tested materials. After 1 h of stabilization at the open-circuit potential, the corrosion potential (E_{corr}) for the AISI 317LMN in the artificial seawater was approximately –0.29 V. Following the Tafel region, the alloy exhibited a broad range of passivation. The breakdown potential (E_b) for the AISI 317LMN in artificial seawater was approximately 1.2 V. In the case of the AISI 316L, the E_{corr} in the artificial seawater was essentially the same as in the case of AISI 317LMN. The range of passivation was significantly narrowed compared to the AISI 317LMN specimen and the E_b was 0.20 V. The corrosion-current densities in the passive range were similar for both the tested specimens.

The cyclic voltammograms of the AISI 317LMN and AISI 316L recorded in the artificial seawater enabled us to ascribe the current-density peaks to the corresponding electrochemical processes taking place on the surface of the investigated materials, and the influence of the potential scan rate (ν) was also studied (**Figures 2 and 3**). The cyclic voltammograms were recorded for the

Table 1: The composition of AISI 317LMN and AISI 316L stainless steels in mass fractions, *w*/%
Tabela 1: Kemijska sestava nerjavnih jekel AISI 317LMN in AISI 316L, masni delež, *w*/%

	w(Cr)	*w*(Ni)	*w*(Mn)	*w*(Si)	*w*(P)	*w*(S)	*w*(C)	w(Mo)
AISI 316L	17.00	10.00	1.40	0.38	0.041	< 0.005	0.021	2.10
AISI 317 LMN	17.33	12.82	1.64	0.39	0.027	< 0.0005	0.014	4.06

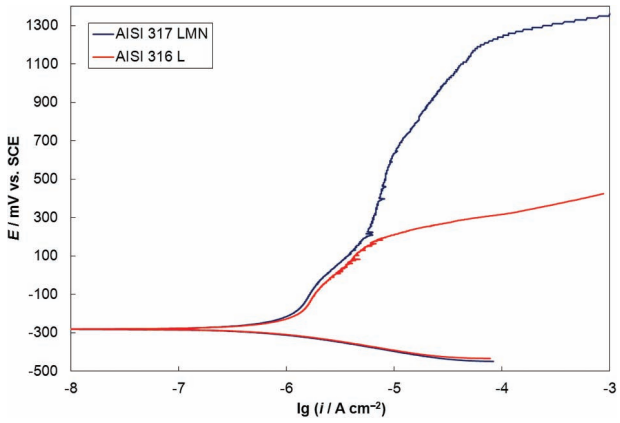

Figure 1: Polarisation curves recorded for AISI 317LMN and AISI 316L stainless steel in 3.5 % NaCl

Slika 1: Polarizacijske krivulje za nerjavni jekli AISI 317LMN in AISI 316L v 3,5-odstotni raztopini NaCl

AISI 316L and AISI 317LMN at different scan rates, in the potential ranges from –1.0 V to 0.4 V and 1.2 V, respectively. In the presence of the artificial seawater four peaks are observed in the cyclic voltammogram for the AISI 317 LMN (**Figure 2**). The first anodic peak A1 at a potential of –0.6 V can be ascribed to the electro-formation of Fe(II) oxide upon the Cr(III)-containing passivating layer, existing on the electrode at such negative potentials according to the reaction: $Fe + H_2O \Leftrightarrow FeO + 2H^+ + 2e^-$ [32]. The second anodic peak A2 at the potential of –0.1 V is ascribed to the oxidation of the Fe(II) species to the Fe(III) species according to the reaction: $2Fe^{2+} + 3H_2O \Leftrightarrow Fe_2O_3 + 6H^+ + 2e^-$ [32]. This is followed by the narrow region with a constant current density, up to 0.5 V, where the current density starts to increase and the transpassive region is reached. In that region the transpassive oxidation of the Cr(III) species to the Cr(VI) species occurs, the Ni(II) species formed

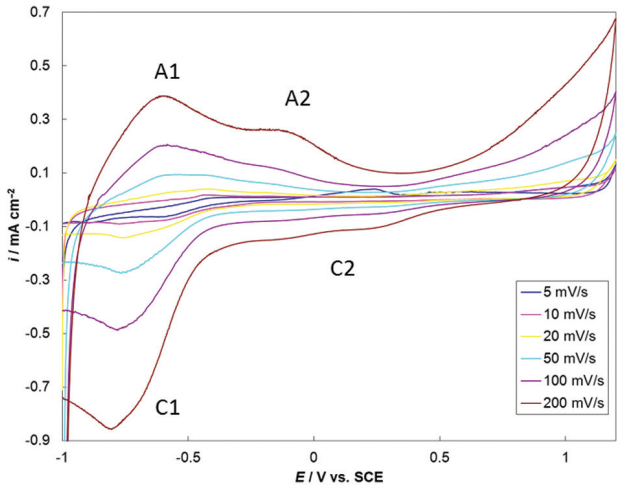

Figure 2: Cyclic voltammograms recorded for AISI 317LMN stainless steel with increasing scan rate in 3.5 % NaCl

Slika 2: Ciklični voltamogrami za nerjavno jeklo AISI 317LMN v 3,5-odstotni raztopini NaCl z naraščajočo hitrostjo spreminjanja potenciala s časom

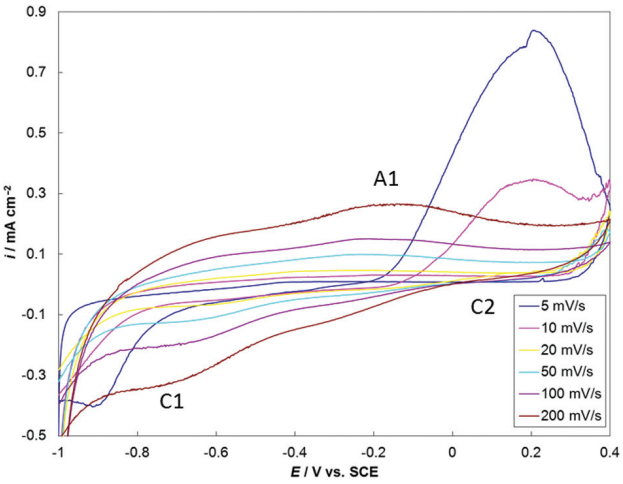

Figure 3: Cyclic voltammograms recorded for AISI 316L stainless steel with increasing scan rate in 3.5 % NaCl

Slika 3: Ciklični voltamogrami za nerjavno jeklo AISI 316L v 3,5-odstotni raztopini NaCl z naraščajočo hitrostjo spreminjanja potenciala s časom

during the passivation process might have been oxidised to Ni(IV) oxide (NiO_2) in this potential range, too [32]. In the reduction cycle in the potential range of peak C2 at 0.2 V the Cr(VI) is reduced to Cr(III) and the iron oxide-hydroxide layer is largely reduced in the potential range of the peak C1 at a potential of –0.8 V [20].

In the case of the AISI 316L in artificial seawater (Figure 3), the anodic peak at a potential of –0.1 V is observed in the cyclic voltammograms and can be ascribed to the electro-formation of Fe(II) oxide. After the passive region the range of the transpassive oxidation is reached at a potential of 0.35 V. In the case of slower scan rates, i.e., 5–10 mV/s, a hysteresis is formed in the reverse cycle, indicating the pronounced dissolution of the oxide layer formed at higher potentials. In the reduction cycle both peaks are less evident on that scale; however, in the potential range of peak C2 at 0.2 V the Cr(VI) is reduced to Cr(III) and the second peak in the cathodic cycle at –0.7 V corresponds to the reduction of the iron oxide-hydroxide layer.

The influence of the scan rate on the oxidation-reduction processes for both investigated materials in cyclic voltammograms is also presented in **Figures 2 and 3**. The current density of the anodic and cathodic peaks increases linearly with the scan rate. The potentials of the anodic and cathodic peaks move slightly, with the increasing scan rate, towards more positive and negative values, respectively.

4 CONCLUSIONS

The corrosion behaviours of the AISI 317LMN and AISI 316L stainless steels were studied in artificial seawater. The study was conducted using the electrochemical techniques of cyclic voltammetry and potentiodynamic measurements.

The potentiodynamic measurements showed the superior corrosion stability of AISI 317 LMN stainless steel in comparison to AISI 316L stainless steel. The range of passivation was significantly broader for the AISI 317LMN compared to the AISI 316L specimen. The corrosion-current densities in the passive range were similar for both the tested specimens.

The cyclic voltammograms revealed the similar electrochemical behaviour of both the tested materials in the presence of the artificial seawater, although in a different potential range. In the case of the AISI 317LMN stainless steel, four peaks were observed corresponding to the electro-formation of the Fe(II) and Fe(III) species, and subsequently to the reduction of Cr(VI) to Cr(III) oxide and the reduction of the iron oxide-hydroxide layer. In the case of the AISI 316L stainless steel the anodic peak was ascribed to the electro-formation of Fe(II) oxide. In the cathodic cycle the reduction of Cr(VI) and the reduction of the iron oxide-hydroxide layer occurs, similar to the results for the AISI 317LMN stainless steel.

The results of the present study show that the electrochemical characteristics of AISI 317LMN and AISI 316L stainless steel are similar. However, the corrosion resistance of AISI 317LMN stainless steel under the investigated conditions is superior compared to AISI 316L, which indicates the possibilities of its application in a marine environment.

5 REFERENCES

[1] C. Donik, I. Paulin, M. Jenko, Mater. Tehnol., 44 (**2010**), 67–72

[2] Y. Wu, U. Nurnberger, Materials and Corrosion-Werkstoffe Und Korrosion, 60 (**2009**), 771–780

[3] A. Kocijan, C. Donik, M. Jenko, Corrosion Science, 49 (**2007**), 2083–2098

[4] A. Kocijan, M. Conradi, Mater. Tehnol., 44 (**2010**), 21–24

[5] D. Mandrino, M. Lamut, M. Godec, M. Torkar, M. Jenko, Surface and Interface Analysis, 39 (**2007**), 438–444

[6] M. Torkar, M. Godec, M. Lamut, Engineering Failure Analysis, 14 (**2007**), 1218–1223

[7] D. Mandrino, M. Godec, A. Kocijan, M. Lamut, M. Torkar, M. Jenko, Metalurgija, 47 (**2008**), 119–123

[8] D. Mandrino, M. Godec, M. Torkar, M. Jenko, Surface and Interface Analysis, 40 (**2008**), 285–289

[9] C. Donik, A. Kocijan, D. Mandrino, I. Paulin, M. Jenko, B. Pihlar, Applied Surface Science, 255 (**2009**), 7056–7061

[10] C. Donik, A. Kocijan, I. Paulin, M. Jenko, Mater. Tehnol., 43 (**2009**), 137–142

[11] C. Donik, A. Kocijan, J. T. Grant, M. Jenko, A. Drenik, B. Pihlar, Corrosion Science, 51 (**2009**), 827–832

[12] M. Godec, A. Kocijan, D. Dolinar, D. Mandrino, M. Jenko, V. Antolic, Biomedical Materials, 5 (**2010**), sp. iss., doi: 10.1088/ 1748-6041/ 5/4/045012

[13] A. Minovic, I. Milosev, V. Pisot, A. Cor, V. Antolic, Journal of Bone and Joint Surgery-British, 83B (**2001**), 1182–1190

[14] A. Kocijan, I. Milosev, B. Pihlar, Journal of Materials Science-Materials in Medicine. 14 (**2003**), 69–77

[15] A. Kocijan, C. Donik, M. Jenko, Mater. Tehnol., 43 (**2009**), 195–199

[16] A. Kocijan, C. Donik, M. Jenko, Mater. Tehnol., 43 (**2009**), 39–42

[17] C. Donik, D. Mandrino, M. Jenko, Vacuum, 84 (**2010**), 1266–1269

[18] A. Kocijan, Mater. Tehnol., 44 (**2010**), 239–242

[19] D. Mandrino, C. Donik, M. Jenko, Surface and Interface Analysis, 42 (**2010**), 762–765

[20] A. Kocijan, D. K. Merl, M. Jenko, Corrosion Science, 53 (**2011**), 776–783

[21] D. A. Skobir, M. Godec, M. Jenko, B. Markoli, Surface and Interface Analysis, 40 (**2008**), 513–517

[22] M. Godec, D. Mandrino, M. Jenko, Engineering Failure Analysis, 16 (**2009**), 1252–1261

[23] D. A. Skobir, M. Godec, M. Balcar, M. Jenko, Vacuum, 84 (**2009**), 205–208

[24] D. A. Skobir, M. Godec, A. Nagode, M. Jenko, Surface and Interface Analysis, 42 (**2010**), 717–721

[25] D. A. Skobir, M. Jenko, D. Mandrino, Surface and Interface Analysis, 36 (**2004**), 941–944

[26] M. Jenko, F. Vodopivec, H. J. Grabke, H. Viefhaus, B. Pracek, M. Lucas, M. Godec, Steel Research, 65 (**1994**), 500–504

[27] P. Sevc, D. Mandrino, J. Blach, M. Jenko, J. Janovec, Kovove Materialy-Metallic Materials, 40 (**2002**), 35–44

[28] J. A. Platt, A. Guzman, A. Zuccari, D. W. Thornburg, B. F. Rhodes, Y. Oshida, B. K. Moore, American Journal of Orthodontics and Dentofacial Orthopedics, 112 (**1997**), 69–79

[29] G. Blanco, A. Bautista, H. Takenouti, Cement & Concrete Composites, 28 (**2006**), 212–219

[30] L. Gil, S. Bruhl, L. Jimenez, O. Leon, R. Guevara, M. H. Staia, Surface & Coatings Technology, 201 (**2006**), 4424–4429

[31] T. Hryniewicz, R. Rokicki, K. Rokosz, Corrosion, 64 (**2008**), 660–665

[32] R. M. Souto, I. C. M. Rosca, S. Gonzalez, Corrosion, 57 (**2001**), 300–306